








Development of a MS compatible HPLC-HILIC method for the analysis of allantoin and glycolic acid in snail slime and related dosage forms: Focus on the enantioseparation of allantoin

Samuele Bonafè^{a,1}, Michele Protti^{b,1} , Andrea Carotti^a, Cinzia Pagano^a ,
Alessandro Di Michele^c , Anna Migni^a , Luana Perioli^a, Laura Mercolini^{b,*} ,
Roccaldo Sardella^{a,**}

^a Department of Pharmaceutical Sciences, University of Perugia, Via Fabretti 48, 06123, Perugia, Italy

^b Department of Pharmacy and Biotechnology (FaBiT), Alma Mater Studiorum, University of Bologna, Via Belmeloro 6, 40126, Bologna, Italy

^c Department of Physics and Geology, University of Perugia, Via Pascoli 1, 06123, Perugia, Italy

ARTICLE INFO

Keywords:

Amylose-based chiral stationary phase
Diol-type stationary phase
Enantioselective analysis
Hydrophilic interaction liquid chromatography
Snail slime-based hydrogel

ABSTRACT

Glycolic acid and allantoin are known to be responsible, at least in part, for the main activities of snail slime, such as moisturizing, skin regeneration, antioxidant, soothing and anti-inflammatory. Accordingly, a hydrophilic interaction liquid chromatography (HILIC) method for the analysis of allantoin and glycolic acid in snail slime samples was developed by a conventional UV–Vis detector and the diol-type Luna® HILIC column. An optimized eluent made up of acetonitrile/water/methanol/formic acid (90:5:5:0.1 v/v/v/v) allowed the separation of the two investigated compounds from each other and from lactic acid and hydantoin used as internal standards. Being allantoin a chiral compound, an enantioselective HPLC protocol was also developed. The chiral analysis of allantoin was performed with the Lux® 3 µm i-Amilose-3 chiral stationary phase using the same mobile phase as for the achiral analysis. The chiral method was efficiently transferred to a HPLC system coupled to triple-quadrupole mass spectrometry (MS/MS). HPLC-MS/MS analysis revealed the racemic nature of allantoin in the pure snail slime. The same profile was also observed in a prototype hydrogel prepared with snail slime. Moreover, the same method allowed to measure the amount of glycolic acid in the two investigated samples (pure snail slime and gel) and ascertain a valuable extraction recovery. The enantiomeric elution order (*S*)<(*R*) with the amylose-based phase was established coupling the results of experimental electronic circular dichroism analysis to time-dependent density functional theory simulations.

1. Introduction

Raw materials from natural sources are very sought and used for the preparation of dermatological and cosmetic products, especially in the development of formulations able to promote skin health through different mechanisms. Among these sources the interest on snail slime potentialities is growing. It is widely used, already for a long time, in many cosmetic products for its softening and eudermic activity but it is known and appreciated mainly for its antiaging activity [1]. However, because of its chemical composition, it could be an interesting active ingredient functional for dermatological products intended to treat

certain skin diseases. In this respect, empirically, the slime of the brown garden snail, *Helix aspersa*, was used since ancient times in human medicine tracing back to the ancient Greeks and Romans [2,3].

The first medical uses were even described by Hippocrates and Galen who prescribed it as an excellent remedy to treat skin inflammation and fluid accumulation (edema). Among the applications, it should be also mentioned its use for the treatment of burn wounds due to its healing capacity.

The composition of snail slime varies by species but typically consists of 90 %–99.7 % water by weight. The remaining components include a mixture of substances such as growth factors, antioxidants, amino acids.

* Corresponding author.

** Corresponding author.

E-mail addresses: laura.mercolini@unibo.it (L. Mercolini), roccaldo.sardella@unipg.it (R. Sardella).

¹ Samuele Bonafè and Michele Protti contributed equally to this work.

Additional constituents found in snail slime include glycosaminoglycans (e.g., hyaluronic acid), glycoproteins (e.g., collagen, elastin), allantoin, glycolic and lactic acids [4]. The unique combination of such ingredients makes snail slime a product with specific peculiarities that can be exploited in health products useful to treat skin diseases [5].

The scientific study of its composition and biological properties allows its use to be reevaluated, explain its many activities and calculate exactly the quantities to be used allowing a safe use as health product laws require.

The main activities are attributable to allantoin (also known as 5-ureidohydantoin, Fig. 1) and glycolic acid (or α -hydroxyacetic acid, Fig. 1) the most abundant molecules found in snail slime. Allantoin is a molecule used in many cosmetic products because of its ability to promote cell proliferation, skin repair [6] as well as for its antioxidant, moisturizing, and soothing effect [7]. Conversely, glycolic acid, is a molecule largely used for peeling, also able to stimulate fibroblasts activity, as well as collagen production and is also involved in inflammatory cytokine modulation [8].

Recent studies highlighted the antimicrobial activity of snail slime exploited in products intended for acne treatment [1], representing a safe alternative to conventional tretinoin-based therapies for which a careful surveillance is necessary [9].

Snail slime ability to stimulate cell (keratinocytes and fibroblast) proliferation and migration makes it a suitable raw material used in topical products such as creams intended for skin repair [10]. The use of snail slime in cosmetic products is well consolidated in EU and extra-EU countries [11]. It is safe to use although it is necessary, for every developed product, to carry out studies to assess possible irritant/allergic effects.

The increasing demand for products based on snail slime and the growing interest in its use in health products create an economic market poised for expansion in the coming years. An analysis of the snail beauty product market estimated its global value at \$457.50 million in 2021, with projections indicating a growth to \$982.70 million by 2031 [12]. The estimated compound annual growth rate stands at 8.3 %, encompassing all product types, applications, and distribution channels.

The content of the two most valuable components, allantoin and glycolic acid (Fig. 1), has been documented to depend on various factors, including the snail species, feeding as well as the growth conditions (soil quality and diet appearing are the most influential) [13]. This means that each snail slime needs to be deeply characterized.

This variability, in terms of the content of such molecules has a significant impact on the quality and effectiveness of dermocosmetic products based on snail slime. Thus, in order to obtain a standardization of the snail slime activity, it is necessary to have an analytical method

capable of allowing an accurate dosage of the most representative molecules contained in the raw material (snail slime). The suitability of such method for the molecules dosing in the final formulation is of paramount importance.

To the best of the authors' knowledge, only one scientific publication [14] has been published to date describing the development, validation, and subsequent use of a reversed-phase (RP) liquid chromatography method for the quantification of allantoin and glycolic acid in both snail slime samples and dermocosmetic preparations. In subsequent studies, quantitative assessment of the two molecules of interest has uniformly relied upon the utilization of this RP-HPLC method. Although the original study demonstrated the accuracy of the developed method, the highly polar nature of the investigated molecules may compromise measurement accuracy when employing RP chromatography stationary phases. There is indeed a risk of polar interferents capable of significantly altering the analysis results.

To mitigate the potential risk, in the present study, we describe the development and application of a hydrophilic interaction liquid chromatography (HILIC) [15] method coupled to both UV detection and mass spectrometry (MS) for the quantitative analysis of allantoin and glycolic acid in snail slime samples. Additionally, since allantoin is a molecule containing a chiral centre, an enantioselective liquid chromatography method has been developed in this study. In this framework, the knowledge of the elution order (EO) of enantiomers was obtained by combining electronic circular dichroism (ECD) analysis with time-dependent density functional theory (TD-DFT)-initiated simulations, according to a well-established protocol [16]. Moreover, this investigation allowed us to determine the enantiomeric composition of allantoin in a commercial snail slime sample as well as in a hydrogel prepared using the same snail slime.

2. Materials and methods

2.1. Chemicals and reagents

Analytical and MS-grade acetonitrile (ACN), methanol (MeOH), ethyl acetate (EtOAc), formic acid, ammonium formate, **the four analytical standards** allantoin, glycolic acid, lactic acid and hydantoin, as well as other solvents used for sample preparation (all analytical grade) were **purchased from Merck Life Science** (Merck KGaA, Darmstadt, Germany).

Helix aspersa Muller snail slime (pH 2.5) was purchased through the appropriate commercial channels. Glycerol and hyaluronic acid sodium salt (NaHy, MW 1500–1800 Da), were purchased by A.C.E.F. s.p.a. (Fiorenzuola d'Arda, PC, Italy).

Mobile phases were degassed with 10 min sonication before use. Water used for the HPLC analyses was purified by using a Milli-Q Plus185 system from Millipore (Milford, MA, USA). Analyte stock solutions (1 mg/mL) were prepared by dissolving suitable amounts of pure powders in MeOH and kept at -20°C when not in use. Working standard mixtures were prepared daily by dilution with mobile phase and all solutions were stored protected from light in amber glass vials certified for mass spectrometry from Waters (Milford, MA, USA).

2.2. Hydrogel preparation

The snail slime-based hydrogel, having the following composition NaHy, 2.0 w/w%; Glycerol, 10.0 w/w%; Snail slime, 88.0 w/w%, was prepared as follows: glycerol was solubilized in the snail slime under magnetic stirring (300 rpm), then NaHy was dispersed in the obtained solution by a mechanical stirrer (IKA, Mechanical Overhead Stirrer, Segrate, Milano) at 400 rpm, room temperature (R.T.) for 12 h in order to obtain the complete polymer swelling.

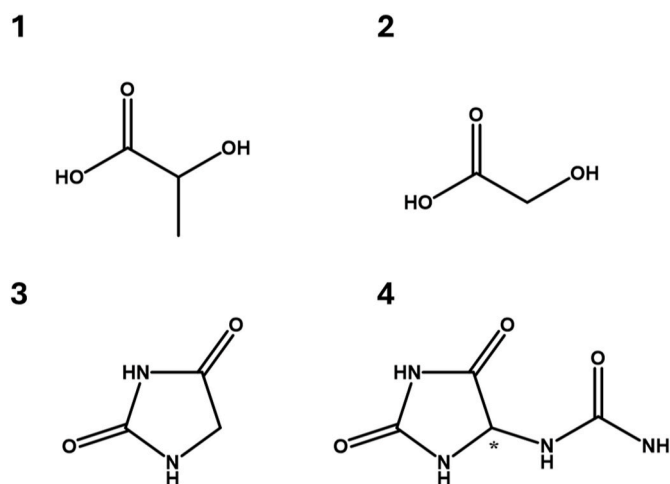


Fig. 1. Chemical structures of 1 - lactic acid, 2 - glycolic acid, 3 - hydantoin, 4 - allantoin.

2.3. Achiral and chiral HPLC-UV analysis

The analytical HPLC measurements for method development were conducted using a Shimadzu (Kyoto, Japan) LC-20A Prominence, equipped with a CBM-20A communication bus module, two LC-20AD dual piston pumps, operated in isocratic mode, an SPD-M20A photodiode array detector, and a Rheodyne 7725i injector (Rheodyne Inc., Cotati, CA, USA) with a 10 μL stainless steel loop. For the optimization of the HILIC-UV method the columns Grom-Sil 120 Diol (Grace, Sedriano, Italy, 250 mm \times 4.6 mm i.d., 5 μm ; SP1) and Luna® HILIC (Phenomenex, USA, 250 mm \times 4.6 mm i.d., 5 μm ; SP2) were comparatively evaluated. The final optimized conditions for the achiral separation of allantoin and glycolic acid are the following: column, SP2; mobile phase, ACN/MeOH/water/formic acid (90:5:5:0.1 v/v/v/v); flow rate, 0.5 mL/min; column temperature, 25 $^{\circ}\text{C}$; wavelength of UV detection, 220 nm.

The chiral separation of allantoin enantiomers was performed on a Shimadzu (Kyoto, Japan) LC-Workstation Class LC-10 equipped with a SCL-10A system controller, a Jasco 880-PU high pressure binary gradient delivery system, a SPD-10A variable-wavelength UV-Vis detector and a Rheodyne 7725i injector (Rheodyne Inc., Cotati, CA, USA) with a 20 μL stainless steel loop. The column temperature was set at 25 $^{\circ}\text{C}$ with a Grace (Sedriano, Italy) heater/chiller (Model 7956R) thermostat. The conditions employed for the enantioselective analysis were the following: column, Lux® 3 μm i-Amilose-3 [Phenomenex, USA, 250 \times 4.6 mm, i.d. 3 μm ; containing the immobilized amylose *tris*(3-chloro-5-methylphenylcarbamate) chiral selector]; mobile phase, ACN/MeOH/water/formic acid (90:5:5:0.1 v/v/v/v); flow rate, 0.5 mL/min; column temperature, 25 $^{\circ}\text{C}$; wavelength of UV detection, 220 nm.

2.4. Achiral and chiral HPLC-MS/MS analysis

The HPLC-MS/MS analysis was carried out using a Waters Alliance e2695 chromatographic system with an autosampler coupled to a Waters Micromass Quattro Micro triple-quadrupole mass spectrometer that was equipped with an electrospray ion source (ESI). The data were processed with Waters MassLynx 4.1 software. Both achiral and chiral separations were obtained using the same stationary and mobile phase combinations exploited for HPLC-UV analysis. Briefly, for non-chiral analysis, the chromatographic column was SP2 (see section 2.3 for details) thermostated at 25 ± 1 $^{\circ}\text{C}$ by means of a Sykam Chromatography (Eresing, Germany) S 4120 column oven. The mobile phase was a mixture composed of ACN/MeOH/water/formic acid (90:5:5:0.1 v/v/v/v) that flowed at a constant rate of 0.5 mL/min and the injection volume was 10 μL . For enantioselective analysis, a Lux® i-Amilose-3 column (250 \times 4.6 mm, i.d. 3 μm) kept at 25 ± 1 $^{\circ}\text{C}$ was exploited together with the same mobile phase as achiral analysis, namely an ACN/MeOH/water/formic acid (90:5:5:0.1 v/v/v/v) mixture flowing at 0.5 mL/min.

An aliquot of 50 μL of snail slime or 10 mg of cosmetic cream sample was dissolved in 1 mL of an ACN/MeOH/water/formic acid (90:5:5:0.1 v/v/v/v) mixture containing hydantoin and lactic acid as internal standards, by magnetic stirring for 10 min at 50 $^{\circ}\text{C}$. The pH of the mixture was adjusted to 3.0, then it was centrifuged at 3400 RPM for 10 min and the supernatant was transferred. In order to purify the mixture from lipophilic matrix components, the mixture was subjected to a miniaturised clean-up protocol exploiting HybridSPE® disposable pipette tips (DPX) from Merck Life Science, optimized ad-hoc to remove potentially interfering phospholipids from the matrices. DPX tips were conditioned by aspirating and discarding 3 times 100 μL of a 1 % (v/v) mixture of formic acid in ACN. Then, an aliquot of 100 μL of sample mixture was loaded by aspirating and dispensing 3 times with the DPX tip. The resulting eluent was collected, and no further sample processing was needed prior to HPLC-MS/MS analysis.

For mass spectrometry, multiple reaction monitoring (MRM) transitions were employed, with both positive and negative ionisation (ESI+, ESI-) in polarity switching mode, using two exclusive transitions for each analyte: the most abundant one for quantitative purposes and

the second for identity confirmation. The optimized parameters were as follows: ion source voltage, 4.0 kV; ion source temperature, 120 $^{\circ}\text{C}$; desolvation temperature, 450 $^{\circ}\text{C}$; desolvation gas flow, 500 L/h (nitrogen as the desolvation gas, argon as the collision gas); dwell time, 300 ms for all compounds. MRM transitions in terms of precursor ions and product ions, cone voltage and collision energy were optimized with SP2 and are shown in Table 1.

2.5. Electronic circular dichroism analysis

The electronic circular dichroism (ECD) spectra were recorded by a Jasco J-810 Spectropolarimeter (Jasco Corporation, Tokyo, Japan) at 25 $^{\circ}\text{C}$, using 10 mm quartz cell. The samples were solubilized in water and analysed in the global spectral range of 190–290 nm.

2.6. Theoretical ECD spectra simulations

The starting structure coordinates of the (S)-allantoin molecule has been retrieved by the crystal structure with pdb code 2q37 [17]. The molecule was then loaded in the Maestro interface (Schrödinger, LLC, New York, NY, 2023) present in the Schrödinger Suite 2023-1; then, the ligprep protocol was adopted to assign the correct protonation state. MMFF94s force field was used to perform a conformational search within the MacroModel module (Schrödinger, LLC, New York, NY, 2023) by executing 200 steps with the “Mixed torsional/Low-mode sampling”, using methanol as solvent and retaining at most 50 conformers, lying in a window of 5.0 kcal mol^{-1} from the global minimum energy.

The torsional sampling involved both multiple Monte Carlo minimum searches for global exploration, and the low mode conformational search allowed for automatic local exploration. The conformers that exceeded the threshold of 0.5 Å of the maximum atom deviation for any pair of corresponding atoms were considered to be different. Following a well-known procedure applied in Ref. [16], the resulting conformers were all submitted to a quantum mechanical energy optimization using the wB97X-D3 as DFT and the 6–311++G**. Finally, the level of accuracy was set to Ultrafine (iacc = 1) in the Jaguar module (Schrödinger, LLC, New York, NY, 2023) [18,19]. A RMSD threshold value of 0.01 Å for heavy atoms was applied to eliminate the high-lying or redundant conformers. The theoretical chiroptical properties of all the compounds were determined using a standard protocol for stereochemical characterization using TD-DFT calculations [20]. The sTD-DFT [21] calculations were carried out using the ORCA 4.1.2 software [22] using the PBE0 as DFT and the TZVP basis set. The 50 lowest energy electronic transitions of each optimized conformer were used to calculate the theoretical values of oscillator strength (f_j), rotational strength in dipole velocity formalism (R_j), and excitation energy (expressed as wavelength, j). By approximation of f_j and R_j values to Gaussian bands with a σ value of 0.3 eV [23], the theoretical spectra of the optimized conformers were then derived. The weighted average of the contribution of all conformers according to their Boltzmann equilibrium populations at 298.15 K and 1 atm (760 mmHg), based on free energy values (G), was

Table 1
Compound-specific MS/MS MRM parameters.

Compound	Parent ion (m/z)	Product ion (m/z) ^a	Cone voltage (V) ^a	Collision energy (eV) ^a
Allantoin	159.09	73.0	19	16
		99.1	19	15
Glycolic acid	75.03	47.2	20	12
		44.9	20	12
Hydantoin	101.04	56.0	20	13
		44.0	20	22
Lactic acid	89.30	42.9	18	10
		40.3	18	20

^a In italic, qualitative MRM data.

used to derive the theoretical ECD spectra of the compound and compared to the experimental spectra. This last step was performed using the SpecDis software [24].

3. Results and discussion

3.1. Optimization of the separation conditions of lactic acid, glycolic acid, hydantoin and allantoin

The primary objective of the chromatographic study was to develop an HPLC method capable of simultaneously quantifying both allantoin and glycolic acid in snail slime samples, followed by a validation procedure. The chromatographic method was initially developed using a conventional HPLC system equipped with a spectrophotometric detector but needed to be easily transferable to HPLC (or UHPLC) instruments coupled with MS. To ensure the method's compatibility with conventional HPLC systems equipped with spectrophotometric detectors, lactic acid and hydantoin (Fig. 1) were included in the samples subjected to chromatographic analysis. Lactic acid was used as a potential internal standard for the quantitative determination of glycolic acid, while hydantoin was used as the internal standard for allantoin quantification. The species hydantoin and lactic acid were selected as internal standards due to their chemical and physicochemical properties, which closely resemble those of allantoin and glycolic acid, respectively.

Given the pronounced polar nature of the four species under investigation, the HILIC (hydrophilic interaction liquid chromatography) mode was considered. Based on a recent study [25] describing the quantitative determination of allantoin in snail slime samples using a HILIC method with a diol stationary phase, this type of column was tested for the separation of the pool of four species under investigation in the present study.

The first step of the study was to compare the chromatographic performance of two diol-type stationary phases (SP1 and SP2, see section 2.3 for details), which are widely used and characterized by specific structural features. SP1 is characterized by linear diols, whereas SP2 is a cross-linked phase incorporating diol functionalities.

The comparative evaluation was conducted using a polar-ionic (PI) mobile phase typical of HILIC applications, consisting of acetonitrile/water/formic acid (95:5:0.1 v/v/v).

All other experimental conditions for the comparison were identical, with the mobile phase flow rate set at 1.0 mL/min and the column temperature maintained at 25 °C. The four compounds were solubilized in the employed eluent.

The two columns, SP1 and SP2, produced the same elution order for the four species (i.e., lactic acid < glycolic acid < hydantoin < allantoin). While the SP1 column exhibited greater retentive capacity than SP2, the latter offered better performance in both thermodynamic and kinetic terms, yielding higher values for separation factor and resolution factor between consecutive peaks (Table 2, entries a and b). The experimental conditions used for comparing the two phases resulted in (i) near-baseline separation between lactic acid and glycolic acid ($R_S = 1.4$); (ii) unsatisfactory resolution between glycolic acid and hydantoin ($R_S = 1.1$; critical resolution R_{S-crit}); and (iii) exceptional resolution between the hydantoin and allantoin peaks ($R_S = 20.2$).

The mobile phase used in the comparative evaluation resulted in reduced solubility of allantoin, which is more soluble in solvents with a higher water content. To address these solubility issues without compromising chromatographic performance due to higher percentages of water in the mobile phase, we replaced 5 % (v/v) of the acetonitrile with an equivalent percentage of methanol, maintaining the aqueous component of the mobile phase unchanged.

To counterbalance the reduced elution efficiency caused by the presence of methanol, characterized by higher solvatochromic power and eluotropic strength, the flow rate was reduced to 0.5 mL/min. This adjustment maintained overall good chromatographic performance while altering the R_{S-crit} , now observed between the peaks of lactic and

Table 2

Chromatographic performance related to the analysis of compounds 1–4 under different experimental conditions (see footnotes for details). k : retention factor; α : separation factor between two consecutive peaks; N : number of theoretical plates; R_S : resolution factor between two consecutive peaks.

Entry	Selected chromatographic parameters				
	Compound	k	α	N	R_S
a	Lactic acid	0.46		4156	
	Glycolic acid	0.54	1.18	n. c.	n. c.
	Hydantoin	0.63	1.16	7779	n. c.
	Allantoin	2.04	3.24	11084	14.94
b	Lactic acid	0.35		12792	
	Glycolic acid	0.42	1.2	10742	1.37
	Hydantoin	0.47	1.13	17007	1.08
	Allantoin	1.77	3.73	17641	20.19
c	Lactic acid	0.26		19692	
	Glycolic acid	0.30	1.16	18580	1.11
	Hydantoin	0.36	1.20	20511	1.55
	Allantoin	1.12	3.14	21970	16.09

a: column, SP1; mobile phase, ACN/water/formic acid (95:5:0.1 v/v/v); flow rate, 1.0 mL/min.

b: Column, SP2; Mobile Phase, ACN/Water/Formic acid (95:5:0.1 v/v/v); Flow rate, 1.0 mL/min.

c: Column, SP2; Mobile Phase, ACN/MeOH/Water/Formic acid (90:5:5:0.1 v/v/v); Flow rate, 0.5 mL/min.

n.c.: not calculated by the software.

glycolic acid (Table 2, entry c).

Other experimental conditions were scrutinized, including further reduction in the eluent flow rate, inclusion of a base or buffer system in the mobile phase to reduce silanophilic activity [26], reduction in formic acid content, substitution of acetonitrile with ethyl acetate [27], and tandem arrangement [28] of SP1 and SP2. However, none of these adjustments yielded significant improvements, with the conditions outlined in Table 2, entry c, deemed optimal. In Fig. 2, the chromatograms in the best identified optimal conditions are shown.

3.2. Enantioseparation of allantoin and determination of the enantiomer elution order through ECD analysis and in silico TD-DFT simulations

Allantoin contains an asymmetric carbon atom, resulting in two enantiomers. (*S*)-Allantoin is reported to be the predominant enantiomer in plants [29–31], while its stereochemistry in snail slime has not been documented. Moreover, irrespective of the natural enantiomeric composition in this matrix, racemization may potentially occur during manufacturing processes. Therefore, developing a method to accurately measure the enantiomeric composition of allantoin in snail slime is of

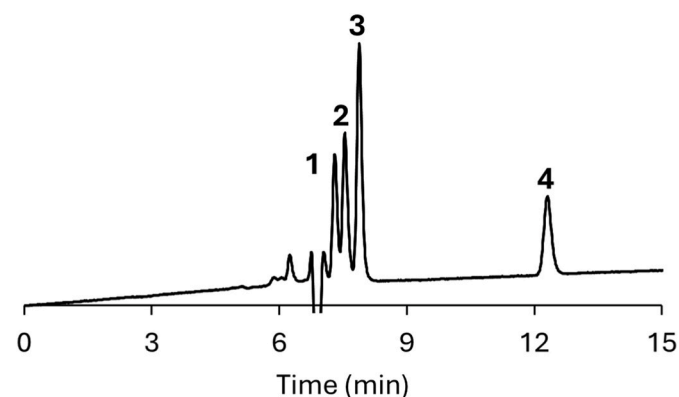


Fig. 2. Chromatogram of a standard mixture of lactic acid (peak 1), glycolic acid (peak 2), hydantoin (peak 3) and allantoin (peak 4). Experimental conditions: Column, SP2; mobile phase, ACN/MeOH/water/formic acid (90:5:5:0.1 v/v/v/v); flow rate, 0.5 mL/min; column temperature, 25 °C; wavelength of UV detection, 220 nm.

primary importance. Aside from a recent study conducted in our laboratories [32], which explored the atypical use of *Cinchona*-alkaloid type zwitterionic chiral stationary phases (CSPs), there are currently no enantioselective LC methods for allantoin analysis reported in the literature. Despite the innovative nature of the developed method, it did not achieve baseline resolution of the two peaks. To address this gap, a new method utilizing an amylose-type CSP (see section 2.3 for details) (Fig. 3) under PI conditions was developed.

In line with the extraordinary versatility and enantioselective capability of polysaccharide-based CSPs under the most relevant elution regimens for LC applications [16,20,33], an extraordinary performance (with $\alpha = 3.1$ and $R_S = 20.2$) was achieved using the optimal eluent system identified during the HILIC study. The utilization of an identical mobile phase in both achiral and chiral chromatographic methods significantly simplify the potential implementation of a two-dimensional chromatography (2D-LC) using a heart-cut approach. This congruence in mobile phase composition minimizes the risk of phase incompatibility and ensures seamless transfer of analytes between the two chromatographic dimensions, thereby enhancing method efficiency and reproducibility.

Fig. 4a presents the chromatogram from the enantioselective chromatography analysis.

Considering the unavailability of pure enantiomeric standards with known stereochemistry, an indirect protocol was employed to determine the enantiomeric excess (EEO) using the employed CSPs under the identified optimal eluent conditions. Following a well-established procedure [16] and given the availability of the x-ray crystallographic structure of the (*S*)-allantoin enantiomer, together with published electronic circular dichroism (ECD) spectra for allantoin enantiomers [17,34,35], allowed us to test the ability of the computational DFT method applied in order to accurately predict the absolute configuration of the two allantoin enantiomers of known absolute configurations. The computed and experimentally measured ECD spectra calculated for the (*R*)- and (*S*)-allantoin enantiomers are shown in Fig. 4.

The excellent chromatographic performance allowed the isolation of sufficient quantities of enantiomers for ECD analysis. This isolation was achieved following a procedure already applied in our laboratory [16], consisting in the repeated injection of the solution containing the racemic mixture for several times (eight times in the present study) at intervals of approximately 25 s. In this manner, two groups of eight peaks were produced, completely separated from each other, resulting in the acquisition of pure enantiomeric species with an enantiomeric excess (*ee*) greater than 99 % (Fig. 4b).

Based on the excellent chromatographic result, the developed enantioselective method is suitable to perform preparative enantioselective analyses [36].

The obtained samples enabled to measure the ECD spectra for the enantiomers of allantoin after peaks collection during the chromatographic runs. As readily evident from Fig. 4c, the experimental and simulated spectra resulted in strict accordance in terms of profiles given Cotton effect signs. In particular the simulated ECD spectra of the (*S*)-allantoin quite well fit the experimental profile of the first eluted peak, thus indicating a (*S*) < (*R*) EEO. In particular the strong positive Cotton effect at around 210 nm, and the slight negative band at λ around 240 nm, are readily evident. A very similar profile has been obtained also by

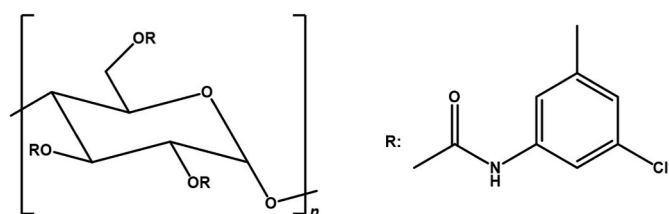


Fig. 3. Structure of the employed amylose-based chiral selector.

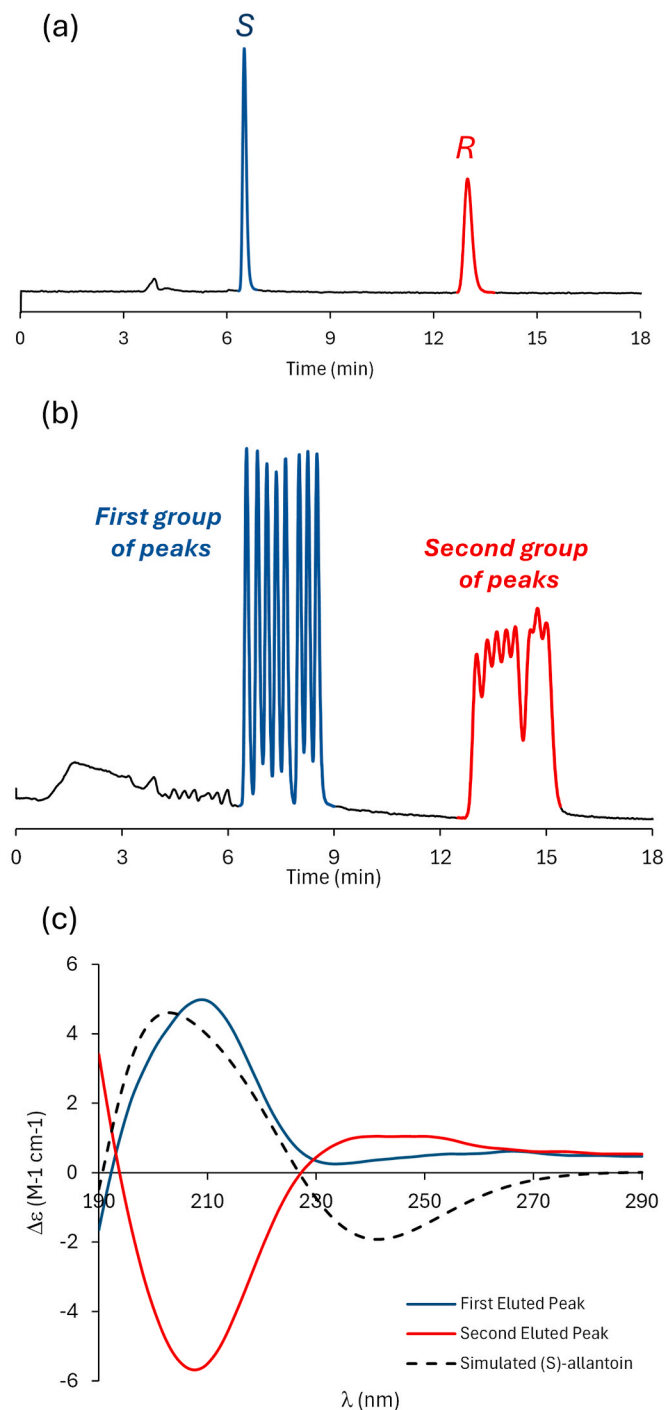


Fig. 4. (a) Chromatogram of racemic allantoin; (b) Chromatographic result of a series of eight consecutive injections of racemic allantoin at intervals of 25 s. Experimental conditions for both chromatograms: Column, Lux® 3 μ m i-Amylose-3 (Phenomenex, USA, 250 \times 4.6 mm, i.d. 3 μ m); mobile phase, ACN/MeOH/water/formic acid (90:5:5:0.1 v/v/v/v); flow rate, 0.5 mL/min; column temperature, 25 $^{\circ}$ C; wavelength of UV detection, 220 nm; (c) Experimental ECD spectra of the first (solid, cyan) and second (solid, orange) eluted peak compared to the simulated spectrum of (*S*)-allantoin (dashed, black).

other authors [31].

3.3. Method application to real samples: HPLC-MS/MS analysis

The developed enantioselective HPLC-MS/MS methodology was exploited for a proof-of-concept application to real samples in order to

quantify allantoin and glycolic acid in pure snail slime and in a formulation in which the snail slime is the main ingredient. With this in mind, the snail slime was formulated in a hydrogel useful for skin application.

Table 3 shows a selection of results obtained from the proof-of-concept method application to real samples by means of the developed HPLC-MS/MS methods. As can be seen, allantoin enantiomers were identified and quantified in the considered samples, together with glycolic acid and added internal standards (hydantoin and lactic acid). In all the cases, the quantitative analysis was carried out with regression curves prepared with standard samples of known concentrations.

As already anticipated in the Introduction section, allantoin is found in a variety of organisms [37], where, as a result of cellular metabolism is produced from the oxidation of uric acid [38], and finally excreted. Even if not specifically investigated for snails, (S)-allantoin has been reported as the sole product of the stereospecific enzymatic reactions involving uric acid, however the racemization of the (S) enantiomer has been demonstrated [39], which can help to explain the situation found in the snail slime object of this study.

4. Conclusions

A HILIC-UV method for the quantification of glycolic acid and allantoin using a diol-type stationary phase under PI conditions was developed. The method is suitable to accurately quantify the two analytes both in snail slime and a snail slime-based hydrogel formulation. Moreover, a chiral HPLC-MS/MS method exploiting an amylose-type polysaccharidic stationary phase was developed, and successfully employed to determine and quantify the presence of both enantiomers of allantoin (as racemate) in the aforementioned matrices.

The chromatographic separations (both achiral and chiral) were optimized on a conventional HPLC-UV system; after that, the methods were easily transferred on LC-MS/MS equipment.

Regarding the enantioseparation study, ECD analysis coupled to TD-DFT simulations allowed to determine the elution order of the two enantiomers.

As a continuation of this work, different samples of snail slime produced in different conditions will be evaluated in terms of allantoin and glycolic acid content. Moreover, the developed HILIC-MS/MS method is intended to be applied to study formulations for skin application such as hydrogels with different compositions, creams, emulgels, polymeric patches.

The development of these precise and accurate analytical methods for health products is very important. In fact, all raw materials used to produce health products (including cosmetic products) as well as finished products are subject to many legislative and regulatory aspects aimed at protecting consumer health. The availability of reliable and practical analytical methods is a valuable aid to quality control for manufacturers, regulators and all actors in the field of pharmacovigilance and/or cosmetovigilance.

CRedit authorship contribution statement

Samuele Bonafè: Writing – original draft, Validation, Methodology, Investigation. **Michele Protti:** Writing – original draft, Validation, Methodology, Investigation. **Andrea Carotti:** Software, Investigation, Formal analysis. **Cinzia Pagano:** Writing – review & editing, Resources. **Alessandro Di Michele:** Investigation, Data curation. **Anna Migni:** Investigation. **Luana Perioli:** Writing – review & editing, Resources. **Laura Mercolini:** Writing – review & editing, Writing – original draft, Visualization, Supervision, Project administration, Methodology, Funding acquisition, Conceptualization. **Roccardo Sardella:** Writing – review & editing, Writing – original draft, Validation, Supervision, Project administration, Methodology, Funding acquisition, Conceptualization.

Table 3

HPLC-MS/MS results from method application to real samples.

Sample	Concentration \pm SD ^a		IS recovery \pm SD (%)		
	Allantoin		Glycolic acid	Hydantoin	Lactic acid
	(S)	(R)			
Pure snail slime	15.9	15.7	2063.6	92.0	88.5
	± 1.6	± 1.5	± 156.7	± 5.4	± 5.3
Snail slime	11.0	10.8	1393.6	88.8	86.7
hydrogel	± 1.1	± 1.2	± 116.9	± 5.8	± 5.8

^a $\mu\text{g/mL}$ for the snail slime sample, $\mu\text{g/g}$ for the snail slime-based hydrogel.

Declaration of competing interest

The authors declare no conflict of interest.

Data availability

Data will be made available on request.

References

- [1] N. Singh, A.N. Brown, M.H. Gold, Snail extract for skin: a review of uses, projections, and limitations, *J. Cosmet. Dermatol.* 23 (2024) 1113–1121, <https://doi.org/10.1111/jocd.16269>.
- [2] G. Cilia, F. Fratini, Antimicrobial properties of terrestrial snail and slug mucus, *J. Complement. Integr. Med.* 15 (2018), <https://doi.org/10.1515/jcim-2017-0168>.
- [3] İ. Ekin, Molluscs: their usage as nutrition, medicine, aphrodisiac, cosmetic, jewelry, cowry, pearl, accessory and so on from the history to today, *Middle East J. Sci.* 4 (2018) 45–51, <https://doi.org/10.23884/mejs.2018.4.1.06>.
- [4] L. Cristiano, M. Guagni, Zoocuticals and cosmetic ingredients derived from animals, *Cosmetics* 9 (2022) 13, <https://doi.org/10.3390/cosmetics9010013>.
- [5] M. Rashad, S. Sampò, A. Cataldi, S. Zara, Biological activities of gastropods secretions: snail and slug slime, *Nat. Prod. Bioprospect.* 13 (2023) 42, <https://doi.org/10.1007/s13659-023-00404-0>.
- [6] Y.D. Nokoorani, A. Shamloo, M. Bahadoran, H. Moravvej, Fabrication and characterization of scaffolds containing different amounts of allantoin for skin tissue engineering, *Sci. Rep.* 11 (2021) 16164, <https://doi.org/10.1038/s41598-021-95763-4>.
- [7] C. Thornfeldt, Cosmeceuticals containing herbs: fact, fiction, and future, *Dermatol. Surg.* 31 (2005) 873–881, <https://doi.org/10.1111/j.1524-4725.2005.31734>.
- [8] C. Egli, M. Min, N. Afzal, R.K. Sivamani, The hydroxy acids: where have we been and what's new? *Dermatol. Rev.* 4 (2023) 260–267, <https://doi.org/10.1002/der2.217>.
- [9] E. Bagatin, C.S. Costa, The use of isotretinoin for acne – an update on optimal dosing, surveillance, and adverse effects, *Exp. Rev. Clin. Pharmacol.* 13 (2020) 885–897, <https://doi.org/10.1080/17512433.2020.1796637>.
- [10] C. Pagano, M.R. Ceccarini, A. Marinelli, A. Imbriano, T. Beccari, S. Primavilla, A. Valiani, M. Ricci, L. Perioli, Development and characterization of an emulgel based on a snail slime useful for dermatological applications, *Int. J. Pharm.* 660 (2024) 124337, <https://doi.org/10.1016/j.ijpharm.2024.124337>.
- [11] Cosmetic ingredient database, https://single-market-economy.ec.europa.eu/sectors/cosmetics/cosmetic-ingredient-database_en, (accessed 29/10/24).
- [12] A. Kamble, R. Deshmukh, Snail beauty products market size, share, competitive landscape and trend analysis report by product type (multi function cream, cell renewal cream, anti aging cream, anti acne cream, others), by application (skin, hair), by distribution channel (hypermarkets and supermarkets, specialty stores, E commerce): global opportunity analysis and industry forecast, 2021–2031, *Allied Market Reports* (2022) 0-270, Report ID: A16873.
- [13] A. Ricci, M. Gallorini, N. Feghali, S. Sampò, A. Cataldi, S. Zara, Snail slime extracted by a cruelty free method preserves viability and controls inflammation occurrence: a focus on fibroblasts, *Molecules* 28 (2023) 1222, <https://doi.org/10.3390/molecules28031222>.
- [14] M.A.S. El Mubarak, F.N. Lamari, C. Kontoyannis, Simultaneous determination of allantoin and glycolic acid in snail mucus and cosmetic creams with high performance liquid chromatography and ultraviolet detection, *J. Chromatogr. A* 1322 (2013) 49–53, <https://doi.org/10.1016/j.chroma.2013.10.086>.
- [15] F. Ianni, L. Pucciarianni, A. Carotti, G. Saluti, S. Moretti, V. Ferrone, R. Sardella, R. Galarini, B. Natalini, Hydrophilic interaction liquid chromatography of aminoglycoside antibiotics with a diol-type stationary phase, *Anal. Chim. Acta* 1044 (2018) 174–180, <https://doi.org/10.1016/j.aca.2018.08.008>.
- [16] R. Sardella, A. Carotti, G. Manfroni, D. Tedesco, A. Martelli, C. Bertucci, V. Cecchetti, B. Natalini, Enantioresolution, stereochemical characterization and biological activity of a chiral large-conductance calcium-activated potassium channel opener, *J. Chromatogr. A* 1363 (2014) 162–168, <https://doi.org/10.1016/j.chroma.2014.06.020>.
- [17] K. Kim, J. Park, S. Rhee, Structural and functional basis for (S)-allantoin formation in the ureide pathway, *J. Biol. Chem.* 282 (2007) 23457–23464, <https://doi.org/10.1074/jbc.M703211200>.

- [18] S. Grimme, J. Antony, S. Ehrlich, H. Krieg, A consistent and accurate *ab initio* parametrization of density functional dispersion correction (DFT-D) for the 94 elements H-Pu, *J. Chem. Phys.* 132 (2010), <https://doi.org/10.1063/1.3382344>.
- [19] F. Weigend, Accurate Coulomb-fitting basis sets for H to Rn, *Phys. Chem. Chem. Phys.* 8 (2006) 1057, <https://doi.org/10.1039/b515623h>.
- [20] B. Cerra, A. Carotti, D. Passeri, R. Sardella, G. Moroni, A. Di Michele, A. Macchiarulo, R. Pellicciari, A. Gioiello, Exploiting chemical toolboxes for the expedited generation of tetracyclic quinolines as a novel class of PXR agonists, *ACS Med. Chem. Lett.* 10 (2019) 677–681, <https://doi.org/10.1021/acsmchemlett.8b00459>.
- [21] C. Bannwarth, S. Grimme, A simplified time-dependent density functional theory approach for electronic ultraviolet and circular dichroism spectra of very large molecules, *Comput. Theor. Chem.* 1040–1041 (2014) 45–53, <https://doi.org/10.1016/j.comptc.2014.02.023>.
- [22] F. Neese, The ORCA program system, *WIREs Comput. Mol. Sci.* 2 (2012) 73–78, <https://doi.org/10.1002/wcms.81>.
- [23] P.J. Stephens, N. Harada, ECD cotton effect approximated by the Gaussian curve and other methods, *Chirality* 22 (2010) 229–233, <https://doi.org/10.1002/chir.20733>.
- [24] T. Bruhn, A. Schaumlöffel, Y. Hemberger, G. Bringmann, SpecDis: quantifying the comparison of calculated and experimental electronic circular dichroism spectra, *Chirality* 25 (2013) 243–249, <https://doi.org/10.1002/chir.22138>.
- [25] T. Deng, D. Gao, X. Song, Z. Zhou, L. Zhou, M. Tao, Z. Jiang, L. Yang, L. Luo, A. Zhou, L. Hu, H. Qin, M. Wu, A natural biological adhesive from snail mucus for wound repair, *Nat. Commun.* 14 (2023) 396, <https://doi.org/10.1038/s41467-023-35907-4>.
- [26] S. Carda-Broch, M.C. García-Alvarez-Coque, M.J. Ruiz-Angel, Extent of the influence of phosphate buffer and ionic liquids on the reduction of the silanol effect in a C18 stationary phase, *J. Chromatogr. A* 1559 (2018) 112–117, <https://doi.org/10.1016/j.chroma.2017.05.061>.
- [27] Y. Shen, B. Chen, T.A. van Beek, Alternative solvents can make preparative liquid chromatography greener, *Green Chem.* 17 (2015) 4073–4081, <https://doi.org/10.1039/C5GC00887E>.
- [28] R. Sardella, M. Lämmerhofer, B. Natalini, W. Lindner, In-line coupling of a reversed-phase column to cope with limited chemoselectivity of a quinine carbamate-based anion-exchange type chiral stationary phase, *J. Separ. Sci.* 31 (2008) 1702–1711, <https://doi.org/10.1002/jssc.200800058>.
- [29] S. Fahad, F.A. Khan, N. Pandupuspitasari, S. Hussain, I.A. Khan, M. Saeed, S. Saud, S. Hassan, M. Adnan, Amanullah, M. Arif, M. Alam, H. Ullah, K.R. Hakeem, H. Alharby, M. Riaz, M. Sameeullah, H.M. Hammad, W. Nasim, S. Ahmad, M. Afzal, S.S. Alghamdi, A.A. Bamagoos, E.F. Abd Allah, J. Huang, Suppressing photorespiration for the improvement in photosynthesis and crop yields: a review on the role of S-allantoin as a nitrogen source, *J. Environ. Manag.* 237 (2019) 644–651, <https://doi.org/10.1016/j.jenvman.2019.02.082>.
- [30] R. Kaur, J. Chandra, B. Varghese, S. Keshavkant, Allantoin: a potential compound for the mitigation of adverse effects of abiotic stresses in plants, *Plants* 12 (2023) 3059, <https://doi.org/10.3390/plants12173059>.
- [31] S. Ding, L. Jia, A. Durandin, C. Crean, A. Kolbanovskiy, V. Shafirovich, S. Broydé, N.E. Geacintov, Absolute configurations of spiroiminodihydantoin and allantoin stereoisomers: comparison of computed and measured electronic circular dichroism spectra, *Chem. Res. Toxicol.* 22 (2009) 1189–1193, <https://doi.org/10.1021/tx900107q>.
- [32] S. Bonafè, C. Pagano, E. Bianconi, L. Mercolini, A. Macchiarulo, L. Perioli, R. Sardella, A. Carotti, Atypical enantioseparation of a non-ionic form of allantoin with Cinchona alkaloid-based zwitterionic chiral stationary phases, *J. Chromatogr. Open* 6 (2024) 100146, <https://doi.org/10.1016/j.jcoa.2024.100146>.
- [33] B. Sechi, A. Dessì, C. Gatti, R. Dallochio, B. Chankvetadze, S. Cossu, V. Mamane, P. Pale, P. Peluso, Unravelling functions of halogen substituents in the enantioseparation of halogenated planar chiral ferrocenes on polysaccharide-based chiral stationary phases: experimental and electrostatic potential analyses, *J. Chromatogr., A* 1673 (2022) 463097, <https://doi.org/10.1016/j.chroma.2022.463097>.
- [34] E.J. s-Gravenmade, G.D. Vogels, C. van Pelt, Preparation, properties and absolute configuration of (-)-allantoin, *Recl. Trav. Chim. Pays-Bas* 88 (1969) 929–939, <https://doi.org/10.1002/recl.19690880806>.
- [35] I. Ramazzina, L. Cendron, C. Folli, R. Berni, D. Monteverdi, G. Zanotti, R. Percudani, Logical identification of an allantoinase analog (puuE) recruited from polysaccharide deacetylases, *J. Biol. Chem.* 283 (2008) 23295–23304, <https://doi.org/10.1074/jbc.M801195200>.
- [36] R. Sardella, F. Ianni, M. Marinuzzi, A. Macchiarulo, B. Natalini, Laboratory-scale preparative enantioseparations of pharmaceutically relevant compounds on commercially available chiral stationary phases for HPLC, *Curr. Med. Chem.* 24 (2017) 796–817, <https://doi.org/10.2174/0929867323666160907111107>.
- [37] R.M. Dinica, C. Sandu, A.V. Dediu Botezatu, A. Cazanevscaia Busuioc, F. Balanescu, M.D. Ionica Mihaila, C.N. Dumitru, B. Furdui, A.V. Iancu, Allantoin from valuable Romanian animal and plant sources with promising anti-inflammatory activity as a nutraceutical ingredient, *Sustainability* 13 (2021) 10170, <https://doi.org/10.3390/su131810170>.
- [38] M.F. Simoyi, E. Falkenstein, K. Van Dyke, K.P. Blemings, H. Klandorf, Allantoin, the oxidation product of uric acid is present in chicken and Turkey plasma, *Comp. Biochem. Physiol. B Biochem. Mol. Biol.* 135 (2003) 325–335, [https://doi.org/10.1016/S1096-4959\(03\)00086-1](https://doi.org/10.1016/S1096-4959(03)00086-1).
- [39] C. Bovigny, M.T. Degiacomi, T. Lemmin, M. Dal Peraro, M. Stenta, Reaction mechanism and catalytic fingerprint of allantoin racemase, *J. Phys. Chem. B* 118 (2014) 7457–7466, <https://doi.org/10.1021/jp411786z>.